

1 **Synthesis and biological activities of the amide derivative of aplog-1, a**  
2 **simplified analog of aplysiatoxin with anti-proliferative and cytotoxic**  
3 **activities**

4  
5 Yusuke Hanaki,<sup>1</sup> Ryo C. Yanagita,<sup>1,2</sup> Takahiro Sugahara,<sup>3</sup> Misako Aida,<sup>3</sup> Harukuni Tokuda,<sup>4</sup>  
6 Nobutaka Suzuki,<sup>4</sup> and Kazuhiro Irie<sup>\*,1</sup>

7 <sup>1</sup>*Division of Food Science and Biotechnology, Graduate School of Agriculture, Kyoto*  
8 *University, Kyoto 606-8502, Japan*

9 <sup>2</sup>*Department of Applied Biological Science, Faculty of Agriculture, Kagawa University,*  
10 *Kagawa 761-0795, Japan*

11 <sup>3</sup>*Center for Quantum Life Sciences, and Department of Chemistry, Graduate School of Science,*  
12 *Hiroshima University, Higashi-Hiroshima 739-8526, Japan*

13 <sup>4</sup>*Department of Complementary and Alternative Medicine, Clinical R & D, Graduate School of*  
14 *Medical Science, Kanazawa University, Kanazawa 920-8640, Japan*

15  
16 Received November 12, 2014; Accepted December 11 , 2014

17  
18 \*Corresponding author. Tel.: +81-75-753-6281; fax: +81-75-753-6284; e-mail:  
19 irie@kais.kyoto-u.ac.jp

20  
21 **Abstract**

22 Aplog-1 is a simplified analog of the tumor-promoting aplysiatoxin with anti-proliferative  
23 and cytotoxic activities against several cancer cell lines. Our recent findings have suggested  
24 that protein kinase C $\delta$  (PKC $\delta$ ) could be one of the target proteins of aplog-1. In the present  
25 study, we synthesized amide-aplog-1 (**3**), in which the C-1 ester group was replaced with an  
26 amide group, to improve chemical stability *in vivo*. Unfortunately, **3** exhibited 70-fold weaker  
27 binding affinity to the C1B domain of PKC $\delta$  than that of aplog-1□ and negligible  
28 anti-proliferative and cytotoxic activities even at 10<sup>-4</sup> M. A conformational analysis and  
29 density functional theory calculations indicated that the stable conformation of **3** differed from  
30 that of aplog-1. Since 27-methyl and 27-methoxy derivatives (**1**, **2**) without the ability to bind  
31 to PKC isozymes exhibited marked anti-proliferative and cytotoxic activities at 10<sup>-4</sup> M, **3** may  
32 be an inactive control to identify the target proteins of aplogs.

33 *Key words:* Aplysiatoxin, Anti-proliferative, Protein kinase C, Tumor promoter

34

35 Aplysiatoxin (ATX) is a potent tumor promoter that has been isolated from the digestive  
36 gland of the sea hare *Stylocheilus longicauda*.<sup>1)</sup> ATX strongly binds to and activates protein  
37 kinase C (PKC) isozymes, as well as 12-*O*-tetradecanoylphorbol 13-acetate (TPA) and  
38 teleocidin B-4.<sup>2,3)</sup> Since PKC is a family of serine/threonine kinases that play pivotal roles in  
39 cellular signal transduction including proliferation, differentiation, and apoptosis,<sup>4-6)</sup> tumor  
40 promoters may become therapeutic agents for intractable diseases such as cancer, Alzheimer's  
41 disease (AD), and acquired immune deficiency syndrome (AIDS). However, difficulties are  
42 associated with their application to therapeutic uses due to their potent tumor-promoting and  
43 inflammatory activities.<sup>7,8)</sup>

44 Bryostatin-1 (bryo-1)<sup>9)</sup> which was isolated from the marine bryozoan *Bugula neritina*, is a  
45 unique PKC activator that does not exhibit tumor-promoting or inflammatory activity. Bryo-1  
46 has been reported to have significant anti-cancer and anti-proliferative activities, and these have  
47 been attributed to activation of the PKC $\delta$  [ ] [ ] [ ] [ ] [ ] [ ] [ ] [ ] [ ] [ ]<sup>10-12)</sup> which plays a tumor suppressor  
48 role and is involved in apoptosis.<sup>13-15)</sup> Bryo-1 is also expected to become a therapeutic  
49 candidate for AD<sup>16)</sup> and AIDS.<sup>17)</sup> Despite its potential as a new medicinal lead, further studies  
50 on its mode of action and structural optimization have been hampered due to its limited  
51 availability from natural sources and synthetic complexity. A functional oriented synthesis of  
52 the simplified analogs of bryo-1 was recently conducted address these issues.<sup>18,19)</sup>

53 As an alternative approach, we developed aplog-1, a simplified analog of ATX.<sup>20)</sup>  
54 Aplog-1, supplied in only 27 steps *via* standard reactions, was not tumor-promoting or  
55 inflammatory, but was anti-proliferative even though it has the skeleton of tumor-promoting  
56 ATX. The anti-proliferative activity of aplog-1 against several cancer cell lines was previously  
57 shown to be similar to that of bryo-1.<sup>20)</sup> Furthermore, aplog-1 behaved in a similar manner to  
58 bryo-1 rather than TPA for the translocation of GFP-tagged PKC $\delta$  using CHO-K1 cells; aplog-1  
59 as well as bryo-1 translocated GFP-tagged PKC $\delta$  to the nuclear membrane and perinuclear  
60 region rather than to the plasma membrane, unlike TPA.<sup>20)</sup> To examine the contribution of  
61 PKC $\delta$  to the anti-proliferative activity of aplog-1, we recently synthesized 27-methyl and  
62 27-methoxy derivatives (**1**, **2**) that lacked the ability to bind to PKC $\delta$  and evaluated their  
63 anti-proliferative activities against 39 human cancer cell lines.<sup>21)</sup> Compounds **1** and **2** only  
64 exhibited weak anti-proliferative activities against all the human cancer cell lines tested,<sup>21)</sup>  
65 suggesting that the activation of PKC $\delta$  was involved in growth inhibitory activities against

66 several cancer cell lines that were at least sensitive to aplog-1.

67 The next step is to evaluate and improve the anti-proliferative activity of aplog-1 *in vivo*.  
68 When a bioactive compound is applied to *in vivo* studies, its chemical stability is critical to the  
69 drug efficacy. Compounds with ester groups are generally susceptible to hydrolysis by  
70 esterases *in vivo*. For example, epothilone B<sup>22)</sup> showed cytotoxicity by inhibiting the  
71 depolymerization of microtubules<sup>23)</sup>, but its efficacy was limited *in vivo* due to its ester group.  
72 Ixabepilone is a derivative of epothilone B, in which the ester group is replaced with an amide  
73 group. Ixabepilone was approved as an anti-breast cancer agent because of its potent  
74 cytotoxicity *in vivo*.<sup>24,25)</sup> Aplog-1 has two ester linkages at C-1 and C-24 in the macrolactone  
75 ring. We previously reported that benzolactams, the simplified analogs of teleocidins, bound  
76 to PKC isozymes more strongly than their lactone counterparts, benzolactones,<sup>26,27)</sup> which  
77 prompted us to develop a new derivative of aplog-1 with a more stable amide linkage. We  
78 herein described the synthesis of amide-aplog-1 (**3**), in which the ester group at C-1 of aplog-1  
79 was replaced with an amide group, along with several of its biological activities such as PKC $\delta$   
80 binding, *in vitro* tumor-promoting, anti-proliferative, and cytotoxic activities. We chose to  
81 replace the C-1 ester group because this site and benzolactones (Figure 1) share a common  
82 hydrophilic substructure, -C(=O)-O-CHR-CH<sub>2</sub>OH, with an inversed stereochemistry, and the  
83 amide proton of **3** was expected to be at a spatial position similar to that of the hydrogen atom  
84 in the hemiacetal 3-OH group of ATX.

85

## 86 **Results and Discussion**

87 The synthesis of **3** was accomplished in a convergent approach from a spiroketal (**6**)<sup>20)</sup>  
88 and carboxylic acid (**5**), as shown in Scheme 1. Compound **4** was prepared from  
89 *Z*-D-Asp(*O**t*Bu)-OH as reported previously<sup>28)</sup> and the subsequent removal of the *t*-butyl ester  
90 with trifluoroacetic acid (TFA) afforded the carboxylic acid (**5**). The spiroketal **6** was  
91 synthesized from *m*-hydroxycinnamic acid in a similar manner to the synthesis of aplog-1.<sup>20)</sup>  
92 Yamaguchi's esterification<sup>29)</sup> of **6** with **5** provided **7**. Oxidative cleavage of the olefin group,  
93 followed by esterification with *N*-hydroxysuccinimide, gave an activated ester. Immediately  
94 after deprotection of the benzyl (Bn) and carbobenzyloxy (Cbz) groups by catalytic  
95 hydrogenation, lactamization occurred to give **3** in a single step. The yield (23% in two steps)  
96 was not good because the Bn group resisted the catalytic hydrogenation.

97 We initially evaluated the ability of **3** to bind to PKC $\delta$  using a synthetic PKC $\delta$ -C1B  
98 peptide ( $\delta$ -C1B),<sup>30)</sup> which is a major binding site and plays a predominant role in the activation

99 of PKC $\delta$  by PKC ligands such as bryo-1, ATX, and TPA. The concentration required to cause  
100 50% inhibition ( $IC_{50}$ ) of [ $^3H$ ]phorbol 12,13-dibutyrate (PDBu) was measured using a  
101 competitive binding assay.<sup>31,32)</sup> Affinity for  $\delta$ -C1B was expressed as a  $K_i$  value calculated from  
102 the  $IC_{50}$  value of **3** and the  $K_d$  value of [ $^3H$ ]PDBu, as reported by Sharkey and Blumberg.<sup>31)</sup>  
103 Table 1 lists the  $K_i$  value of **3** for  $\delta$ -C1B along with those of aplog-1 and its 27-methyl and  
104 27-methoxy derivatives (**1** and **2**). As previously reported,<sup>21,33)</sup> the stereochemistry at position  
105 27 was critical for PKC binding, and the free hydroxyl group at position 27 was indispensable.  
106 Although the amide analog **3** fulfilled these structural requirements at position 27 for PKC $\delta$   
107 binding, the affinity of **3** ( $K_i = 520$  nM) was approximately two orders of magnitude weaker  
108 than that of aplog-1 ( $K_i = 7.4$  nM).

109       Regarding PKC activators such as 1,2-diacyl-*sn*-glycerol (DAG) and indolactam-V (Fig.  
110 1), the replacement of an ester group with an amide group and *vice versa* significantly affected  
111 their abilities to bind to PKC isozymes by changing their conformation. The replacement of  
112 either the *sn*-1 or *sn*-2 ester group of DAG, an endogenous second messenger, with an amide  
113 group markedly reduced its ability to activate PKC isozymes.<sup>34)</sup> The conformationally  
114 constrained analogs of DAG (DAG-lactones) with similar modifications developed by Marquez  
115 and colleagues also showed approximately ninety to two hundred-fold lower binding affinities  
116 for PKC $\alpha$  than those of their ester counterparts.<sup>35)</sup> On the other hand, amide-to-ester  
117 modification in the indolactam-V analogs gave opposite results. A lactone analog of the  
118 nine-membered indolactam-V, the core structure of teleocidins, showed a different  
119 conformational preference and was completely inactive,<sup>36)</sup> while a lactone analog of the  
120 eight-membered benzolactam-V8 took a ring conformation similar to that of benzolactam-V8  
121 with *cis*-amide, and exhibited twenty to ninety-fold lower affinity for PKC C1 domains than the  
122 corresponding benzolactam-V8 analog.<sup>27)</sup> Therefore, both ester and amide analogs could bind  
123 to PKC isozymes if it adopted an appropriate conformation.

124       The strong binding ability of ATX to PKC isozymes was attributed to the rigid  
125 conformation of the macrocyclic ring, which included a hydrophilic pharmacophore,<sup>33)</sup> and an  
126 NMR analysis of aplog-1<sup>20)</sup> indicated that its preferred macrocyclic ring conformation was  
127 similar to that of 3-deoxy-debromo-ATX (*e.g.*,  $J_{2,3} = 10.8$  and 2.8 Hz for aplog-1; 11 and 3 Hz  
128 for 3-deoxy-debromo-ATX).<sup>33)</sup> In the case of **3**, an nOe correlation between NH-26 and H-11  
129 was observed in a 2D NOESY NMR experiment in CDCl $_3$  (Supplemental Fig. 2), suggesting  
130 that the conformation of **3** differed to those of ATX<sup>33)</sup> and aplog-1, in which the distance  
131 between these atoms could be more than 4 Å. Since ATX and aplogs were involved in the

132 hydrophobic environment when bound to PKC $\delta$ -C1B in the presence of phosphatidylserine, the  
133 conformation of **3** in CDCl<sub>3</sub> would reflect a conformation in a ternary complex of **3**, PKC $\delta$ -C1B,  
134 and phosphatidylserine membrane. In order to clarify the effects of conformational changes in  
135 **3** on decreases in PKC $\delta$  binding, we performed a conformational search followed by density  
136 functional theory (DFT) calculations to estimate the relative stabilities of possible conformers.

137 A set of possible conformations of the macrolactone core structure of **3** was generated by  
138 the simulated annealing method, and we chose three possible conformers: the global-minimum  
139 with a *trans*-amide, an ATX-like conformation with a *trans*-amide, and a conformation with a  
140 *cis*-amide because the active conformation of indolactam compounds is known to be a *cis*-amide  
141 form.<sup>37,38</sup> Side chains at C-11 were attached to them and dihedral angles in the side chain  
142 were manually rotated to search for an energetically stable orientation, in which the 18-OH  
143 group is involved in intramolecular hydrogen bonding as suggested by its sharp <sup>1</sup>H NMR signal  
144 in CDCl<sub>3</sub>. The candidate structures were pre-optimized using the molecular mechanics method  
145 with the MMFF94s force field and the final DFT geometry optimizations were then performed  
146 at the  $\omega$ B97X-D/6-31G\* level of theory.<sup>39</sup> Figure 2 shows the resulting three possible  
147 conformers of **3** (**A-C**) and their relative  $\omega$ B97X-D/6-31G\* energies.

148 As described above, conformers **A** and **B** had a *trans*-amide bond, while **C** had a *cis* one.  
149 Conformer **B** resembles a stable conformation of ATX.<sup>33</sup> In conformers **A** and **B**, NH-26 and  
150 H-11 were spatially close (2.06 Å in **A**, 2.61 Å in **B**), which is consistent with the nOe  
151 correlation. Furthermore, the sharp and downfield-shifted <sup>1</sup>H NMR signal of NH-26 (7.45  
152 ppm) in CDCl<sub>3</sub> could be explained by intramolecular hydrogen bonding between N-H and an  
153 oxygen atom in these conformers. DFT calculations showed that conformer **A** had the lowest  
154 energy, and differences in energies between **A-B** and **A-C** were 1.365 and 13.259 kcal mol<sup>-1</sup>,  
155 respectively. These results suggested that **3** existed as conformer **A** in CDCl<sub>3</sub>. Since  
156 conformer **B** resembled but significantly diverged from the stable conformation of ATX due to  
157 the rotation of amide plane by 45° (based on N—C-1—C-2—C-3 dihedral angle), the difference  
158 in energies between conformer **A** and the ATX-like active conformation would be more than  
159 1.365 kcal mol<sup>-1</sup>. Thus, a 70-fold decrease in the binding ability of **3** from aplog-1, which is  
160 equivalent to a 2.34 kcal mol<sup>-1</sup> change in free energy, could be ascribable mainly to the change  
161 in the conformational preference.

162 We then evaluated the tumor-promoting activity of **3** *in vitro* by testing the induction of  
163 Epstein-Barr virus early antigen (EBV-EA) production.<sup>40,41</sup> EBV is activated by treating cells  
164 with tumor promoters such as TPA in order to produce EA, which can be detected by an indirect

165 immunofluorescence technique. Aplog-1 and its C-27 derivatives (**1** and **2**) induced EA  
166 production more weakly than the potent tumor promoter TPA. The ability of **3** to induce EA  
167 production was weaker than those of **1** and **2** without the ability to bind to PKC  
168 isozymes<sup>21,33</sup> Figure 3 Although EA production is considered to be related to the  
169 activation of PKC isozymes,<sup>42</sup> this result suggested that some part of the induction of EA  
170 caused by aplog-1 and its derivatives could be attributed to other mechanisms.

171 The anti-proliferative activity of **3** was evaluated with a panel of 39 human cancer cell  
172 lines established by Yamori and colleagues<sup>44,45</sup> The results for HBC-4 and NCI-H460 were  
173 shown in Figure 4 as typical examples, because aplog-1 showed stronger growth inhibitory  
174 activity against these cell lines. Similar results were observed in MDA-MB-231, SNB-78,  
175 HCC2998, A549, LOX-IMVI, and St-4 cell lines (Supplemental Table 1). Cell growth was  
176 estimated by the sulforhodamine B assay and expressed as a percentage of the control without **3**.  
177 As expected from the weak binding affinity for PKC $\delta$ , **3** hardly inhibited their growth at low  
178 concentrations ( $< 10^{-5}$  M) as well as **1** and **2**. Furthermore, **3** exhibited weak cytotoxicity even  
179 at  $10^{-4}$  M, whereas aplog-1, **1**, and **2** induced cell death regardless of their binding affinities for  
180 PKC $\delta$  the same  $10^{-4}$  M. This result suggests that other  
181 targets may be involved in the cytotoxicity of aplogs at  $10^{-4}$  M.

182 In summary, we synthesized a new amide derivative of aplog-1 (**3**) in order to improve  
183 the stability of aplog-1 against esterases and pH changes *in vivo*. Although the very weak  
184 binding of **3** to the C1B domain of PKC $\delta$  could be detected, **3** showed weak anti-proliferative  
185 activity against the 39 cancer cell lines examined, even at  $10^{-4}$  M (Supplemental Table 1), and  
186 hardly induced the production of EBV-EA. In contrast, aplog derivatives without binding  
187 affinity to PKC $\delta$  and its isozymes (**1**, **2**)<sup>21</sup> retained these activities at  $10^{-4}$  M. These results  
188 suggest that some of the anti-proliferative and cytotoxic activities of aplogs were attributed to  
189 unidentified targets other than PKC isozymes. A conformational analysis and DFT  
190 calculations indicated that the stable conformation of **3** differed from that of aplog-1. This  
191 conformational change could prevent **3** from binding to PKC $\delta$  and other target proteins  
192 responsible for anti-proliferative activity and EBV-EA induction. Given that conformational  
193 changes in PKC ligands could affect not only biological activities, but also cellular targets, these  
194 effects must be taken into account to successfully derivatize the skeletons of aplogs in the  
195 future.

196 We recently developed aplog-based molecular probes and are currently attempting to  
197 identify its target proteins other than PKC isozymes. As described above, 27-methyl and

198 27-methoxy derivatives (**1**, **2**) did not exhibit the ability to bind to PKC isozymes, but had  
199 marked anti-proliferative and cytotoxic activities at  $10^{-4}$  M, indicating that **1** and **2** were not  
200 suitable as inactive controls for the target analysis. Since **3** exhibited weak binding affinity for  
201 PKC, but little cytotoxic activity even at  $10^{-4}$  M, it would be suitable as an inactive control for  
202 the identification of targets other than PKC isozymes.

203

204

## 205 **Experimental**

206

207 The following spectroscopic and analytical instruments were used: digital polarimeter,  
208 DIP-1000 (Jasco, Tokyo, Japan);  $^1\text{H}$  and  $^{13}\text{C}$  NMR, Avance III 400, Avance III 500, and Avance  
209 II 800 (reference TMS, Bruker, Germany); HPLC, model 600E with a model 2487 UV detector  
210 (Waters, Tokyo, Japan); and HR-FAB-MS, JMS-600H (JEOL, Tokyo, Japan) and JMS-700  
211 (JEOL, Tokyo, Japan). HPLC was carried out on a YMC-packed ODS-A AA12S05-2510WT  
212 (Yamamura Chemical Laboratory, Kyoto, Japan). Wakogel® C-200 (silica gel, Wako Pure  
213 Chemical Laboratory, Osaka, Japan) was used for column chromatography. [ $^3\text{H}$ ]PDBu (18.7  
214 Ci/mmol) was custom-synthesized by Perkin-Elmer Life Sciences Research Products (Boston,  
215 MA). The PKC $\delta$  C1B peptide was synthesized as reported previously.<sup>30</sup> All other chemicals  
216 and reagents were purchased from chemical companies and used without further purification.

217

218 *Synthesis of 3.* Compound **4** was prepared as reported previously.<sup>28</sup>  $[\alpha]_{\text{D}} +13.2^\circ$  ( $c = 0.44$ ,  
219 MeOH,  $10.9^\circ\text{C}$ ). TFA (0.9 mL) was added to a solution of **4** (35.8 mg,  $89.7\ \mu\text{mol}$ ) in  
220 dichloromethane (0.9 mL) at  $0^\circ\text{C}$ . After 4 h of stirring at room temperature, the reaction  
221 mixture was concentrated *in vacuo* to afford **5** (29.3 mg,  $85.4\ \mu\text{mol}$ , 95%) as a clear oil.  $^1\text{H}$   
222 NMR (500 MHz,  $\text{CDCl}_3$ , 0.015 M) ppm:  $\delta$  2.70 (2H, d,  $J = 5.9$  Hz), 3.55-3.59 (2H, m), 4.23  
223 (1H, br. s), 4.50 (2H, s), 5.09 (2H, s), 5.41 (1H, br. d,  $J = 8.1$  Hz), 7.27-7.37 (10H, m);  $^{13}\text{C}$  NMR  
224 (125 MHz,  $\text{CDCl}_3$ , 0.015 M) ppm:  $\delta$  35.8, 47.8, 66.9, 70.8, 73.4, 127.7 (2C), 127.9 (2C), 128.1,  
225 128.2, 128.5 (2C), 128.6 (2C), 136.4, 137.7, 155.9, 174.1; HR-EI-MS  $m/z$ : 343.1427 ( $[\text{M}]^+$   
226 Calcd. for  $\text{C}_{19}\text{H}_{21}\text{NO}_5$  343.1420)  $[\alpha]_{\text{D}} +16.1^\circ$  ( $c = 0.15$ ,  $\text{CHCl}_3$ ,  $10.3^\circ\text{C}$ ).

227 2,4,6-trichlorobenzoyl chloride (28.0  $\mu\text{L}$ ,  $179\ \mu\text{mol}$ , 1.7 equiv.) was added to a solution of  
228 **5** (51.1 mg,  $149\ \mu\text{mol}$ , 1.4 equiv.) and  $\text{Et}_3\text{N}$  (24.9  $\mu\text{L}$ ,  $179\ \mu\text{mol}$ , 1.7 equiv.) in toluene (1.1 mL)  
229 at room temperature. After 3 h of stirring at room temperature, the supernatant of the  
230 suspension was added to a solution of **6**<sup>20</sup> (50.0 mg,  $105\ \mu\text{mol}$ ) and DMAP (27.0 mg,  $221\ \mu\text{mol}$ ,

231 2.1 equiv.) in toluene (1.1 mL) at room temperature. The mixture was stirred at 50 °C for 2 h  
232 and then poured into H<sub>2</sub>O (5.0 mL). The mixture was extracted with EtOAc (5 mL x 3). The  
233 combined organic layers were washed with brine, dried over Na<sub>2</sub>SO<sub>4</sub>, filtered, and concentrated  
234 *in vacuo*. The residue was purified by column chromatography (silica gel, 10% → 20%  
235 EtOAc/hexane) to afford **7** (67.8 mg, 84.4 μmol, 80%) as a clear oil. <sup>1</sup>H NMR (500 MHz,  
236 CDCl<sub>3</sub>, 0.0027 M) ppm: δ 0.86 (3H, s), 0.95 (3H, s), 1.33-1.49 (9H, m), 1.57-1.66 (4H, m), 2.19  
237 (1H, br. d, *J* = 15.5 Hz), 2.26 (1H, m), 2.35 (1H, m), 2.57 (2H, t, *J* = 7.8 Hz), 2.61 (1H, dd, *J* =  
238 15.8, 8.0 Hz), 2.69 (1H, dd, *J* = 5.8 Hz), 3.49-3.60 (4H, m), 4.16-4.21 (2H, m), 4.47-4.52 (2H,  
239 m), 4.95-5.02 (2H, m), 5.04 (2H, s), 5.06-5.09 (3H, m), 5.56 (1H, br. d, *J* = 8.8 Hz), 5.80 (1H,  
240 m), 6.78-6.82 (3H, m), 7.18 (1H, t, *J* = 7.8 Hz), 7.27-7.45 (14H, m) ; <sup>13</sup>C NMR (125 MHz,  
241 CDCl<sub>3</sub>, 0.0027 M) ppm: δ 22.0, 24.8, 25.3, 26.1, 27.2, 31.3, 33.7, 34.5, 35.6, 36.0, 36.5, 36.8,  
242 40.9, 48.0, 63.9, 66.7, 68.4, 70.0, 71.1, 71.7, 73.3, 100.1, 111.8, 115.2, 116.6, 121.2, 127.5 (2C),  
243 127.6 (2C), 127.8, 127.9 (2C), 128.1, 128.1, 128.4 (2C), 128.5 (2C), 128.6 (2C), 129.2, 135.4,  
244 136.6, 137.3, 137.9, 144.6, 155.8, 158.9, 171.3; HR-FAB-MS (matrix, *m*-nitrobenzyl alcohol)  
245 *m/z*: 826.4324 ([M+Na]<sup>+</sup> Calcd. for C<sub>50</sub>H<sub>61</sub>NO<sub>8</sub>Na 826.4295) [α]<sub>D</sub> +19.7° (*c* = 0.14, CHCl<sub>3</sub>, 28.9  
246 °C).

247 KMnO<sub>4</sub> (13.1 mg, 83.2 μmol, 1 equiv.) was added to a suspension of NaIO<sub>4</sub> (143 mg,  
248 0.666 mmol, 8 equiv.) in pH 7.2 phosphate buffer (6.9 mL) in one portion. After 5 min of  
249 stirring at room temperature under an Ar atmosphere, the mixture was added to a solution of **7**  
250 (66.8 mg, 83.2 μmol) in *t*-BuOH (6.9 mL). The reaction mixture was stirred at room  
251 temperature for 1 h, and the reaction was quenched with Na<sub>2</sub>S<sub>2</sub>O<sub>3</sub> (39.5 mg). The organic layer  
252 was separated, and the aqueous layer was extracted with EtOAc (20 mL x 3). The combined  
253 organic layer were washed with brine, dried over Na<sub>2</sub>SO<sub>4</sub>, filtered, and concentrated *in vacuo*.  
254 The residue was purified by column chromatography (silica gel, 20% EtOAc/hexane containing  
255 1% AcOH) to afford a carboxylic acid (50.8 mg, 61.9 μmol, 74%) as a clear oil.

256 *N,N'*-dicyclohexylcarbodiimide (7.3 mg, 35.4 μmol, 1.5 equiv.) in MeCN (0.20 mL) was  
257 added to a solution of the carboxylic acid (19.4 mg, 23.6 μmol) and *N*-hydroxysuccinimide (5.4  
258 mg, 47.2 μmol, 2 equiv.) in MeCN (0.20 mL) at 0 °C. The reaction mixture was stirred at 0 °C  
259 for 10 h, then concentrated *in vacuo*. The residue was purified by column chromatography  
260 (silica gel, 5% → 10% → 20% → 30 % EtOAc/hexane) to afford a crude activated ester  
261 (28.1 mg). A solution of the activated ester (26.7 mg) in MeOH (1.0 mL) was added to 20%  
262 Pd(OH)<sub>2</sub>-C (wet support, Aldrich) (7.8 mg) in a flask at room temperature. The mixture was  
263 vigorously stirred under a H<sub>2</sub> atmosphere at room temperature for 4.5 h. The mixture was



264 filtered and the filtrate was concentrated *in vacuo*. The residue was dissolved in MeOH (0.6  
265 mL), and again added to 20% Pd(OH)<sub>2</sub>-C (wet support, Aldrich) (5.9 mg) in a flask at room  
266 temperature. The mixture was vigorously stirred under a H<sub>2</sub> atmosphere at room temperature  
267 for 2.5 h. The mixture was filtered and the filtrate was concentrated *in vacuo*. This  
268 procedure was repeated two times and a total of 38.5 mg (46.9 μmol) of the carboxylic acid was  
269 reacted. These residues were purified by HPLC (column, YMC-Pack ODS-A  
270 AA12S05-2510WT; solvent MeOH/H<sub>2</sub>O = 75:25, flow rate 3.0 mL/min; pressure, 2100 psi; UV  
271 detector 254 nm; retention time, 20.1 min) to afford **3** (5.2 mg, 10.6 μmol, 23%) as a clear oil.  
272 <sup>1</sup>H NMR (400 MHz, CDCl<sub>3</sub>, 0.0036 M) ppm: δ 0.96 (3H, s, H<sub>3</sub>-23), 1.00 (3H, s, H<sub>3</sub>-22),  
273 1.38-1.59 (9H, m, H<sub>2</sub>-4, H<sub>2</sub>-5, H-10a, H<sub>2</sub>-12, H<sub>2</sub>-13), 1.64 (2H, m, H<sub>2</sub>-14), 1.71 (1H, dd, *J* = 15.5,  
274 3.7 Hz, H-8α), 1.79 (1H, m, H-10b), 2.28 (1H, dd, *J* = 15.1, 1.1 Hz, H-2a), 2.46 (1H, m, H-8β),  
275 2.55-2.65 (4H, m, H-2b, H<sub>2</sub>-15, H-25a), 2.95 (1H, dd, *J* = 16.5, 10.7 Hz, H-25b), 3.70-3.87 (4H,  
276 m, H-3, H-26, H<sub>2</sub>-27), 4.09 (1H, m, H-11), 4.45 (1H, dd, *J* = 7.6, 5.0 Hz, OH), 5.21 (1H, m,  
277 H-9), 6.27 (1H, s, Ph-OH), 6.65-6.74 (3H, m, H-17, H-19, H-21), 7.13 (1H, t, *J* = 7.8 Hz, H-20),  
278 7.45 (1H, br. d, *J* = 4.7 Hz, NH); <sup>13</sup>C NMR (125 MHz, CDCl<sub>3</sub>, 0.0029 M) ppm: δ 21.5 (C-22),  
279 24.2 (C-13), 25.6 (C-8), 25.9 (C-23), 27.8 (C-4), 30.2 (C-14), 34.2 (C-5 or 10 or 12), 34.4 (C-5  
280 or 10 or 12), 34.7 (C-5 or 10 or 12), 35.3 (C-15), 36.3 (C-25), 37.3 (C-6), 43.8 (C-2), 51.6  
281 (C-26), 63.9 (C-11), 64.5 (C-27), 68.5 (C-9), 71.3 (C-3), 101.3 (C-7), 112.8 (C-19), 115.1  
282 (C-17), 120.6 (C-21), 129.4 (C-20), 144.4 (C-16), 156.3 (C-18), 170.3 (C-24), 173.4 (C-1);  
283 HR-FAB-MS (matrix, *m*-nitrobenzyl alcohol) *m/z*: 490.2812 ([M+H]<sup>+</sup> Calcd. for C<sub>27</sub>H<sub>40</sub>NO<sub>7</sub>  
284 490.2805) [α]<sub>D</sub> +38.9° (*c* = 0.074, CHCl<sub>3</sub>, 9.6 °C).

285

286 *Inhibition of specific binding of [<sup>3</sup>H]PDBu to the PKCδ-C1B peptide.* The binding of  
287 [<sup>3</sup>H]PDBu to the δ-C1B peptide was evaluated by the procedure of Sharkey and Blumberg<sup>31)</sup>  
288 with modifications as reported previously<sup>32)</sup> using 50 mM Tris-maleate buffer (pH 7.4 at 4 °C),  
289 13.8 nM δ-C1B peptide, 20 nM [<sup>3</sup>H]PDBu (18.7 Ci/mmol), 50 μg/mL  
290 1,2-dioleoyl-*sn*-glycero-3-phospho-L-serine sodium salt (Sigma), 3 mg/mL bovine γ-globulin,  
291 and various concentrations of an inhibitor. Binding affinity was evaluated based on the  
292 concentration required to inhibit the specific binding of [<sup>3</sup>H]PDBu by 50%, the IC<sub>50</sub>, which was  
293 calculated by a computer program with a probit procedure.<sup>46)</sup> The inhibition constant, *K<sub>i</sub>*, was  
294 calculated by the method of Sharkey and Blumberg.<sup>31)</sup>

295

296 *EBV-EA induction test.* Human B-lymphoblastoid Raji cells (5 × 10<sup>5</sup>/mL) were incubated at

297 37 °C under a 5% CO<sub>2</sub> atmosphere in 1 mL of RPMI 1640 medium (supplemented with 10%  
298 fetal bovine serum) with 4 mM sodium *n*-butyrate (a synergist) and 10, 100, or 1000 nM of each  
299 test compound. Each test compound was added as 2 μL of a DMSO solution (5, 50, and 500  
300 μM stock solution) along with 2 μL of DMSO; the final DMSO concentration was 0.4%.  
301 After 48 h of incubation, smears were made from the cell suspension, and the  
302 EBV-EA-expressing cells were stained by a conventional indirect immunofluorescence  
303 technique with the serum of an NPC patient's (a gift from Kobe University, Japan) and  
304 FITC-labeled anti-human IgG (DAKO, Glostrup, Denmark) as reported previously.<sup>41)</sup> At least  
305 500 cells were counted in each assay and the proportion of EA-positive cells was recorded.  
306 Cell viability exceeded 60% in all experiments.

307

308 *Measurements of cell growth inhibition.* A panel of 39 human cancer cell lines established by  
309 Yamori and colleagues<sup>44)</sup> according to the NCI method with modifications was employed, and  
310 cell growth inhibitory activity was measured as reported previously.<sup>45)</sup> In brief, cells were  
311 plated on 96-well plates in RPMI 1640 medium supplemented with 5% fetal bovine serum and  
312 allowed to attach overnight. The cells were incubated with each test compound for 48 h.  
313 Cell growth was estimated by the sulforhodamine B assay. Absorbance for the control well  
314 (*C*) and test well (*T*) was measured at 525 nm along with that for the test well at time 0 (*T*<sub>0</sub>).  
315 Cell growth inhibition (% growth) by each concentration of the drug (10<sup>-8</sup>, 10<sup>-7</sup>, 10<sup>-6</sup>, 10<sup>-5</sup>, and  
316 10<sup>-4</sup> M) was calculated as 100[(*T* - *T*<sub>0</sub>)/ (*C* - *T*<sub>0</sub>)] using the average of duplicate points.

317

318 *Conformational search of 3.* The generation of a conformer library of **3** by a simulated  
319 annealing method under a vacuum was performed using the GROMACS program<sup>47)</sup> (version  
320 4.6.5) with a general AMBER force field (GAFF).<sup>48)</sup> The side chain at C11 of **3** was replaced  
321 with a methyl group. All bonds were constrained using the LINCS algorithm. The annealing  
322 temperature was initially set to 1,500 K in order to surpass the *cis-trans* isomerization barrier in  
323 this system and the temperature was kept constant for 1 ps. The temperature was linearly  
324 dropped to 100 K over 1 ps and then to 0 K over 1 ps, and kept at the same temperature for 1 ps.  
325 This 5-ps cycle was repeated 200 times to give the conformer library.

326 Three possible conformers were selected from this library: the global-minimum with  
327 *trans*-amide, ATX-like conformation with *trans*-amide, and a conformation with *cis*-amide.  
328 The side chains at C-11 were attached to them and dihedral angles in the side chain were  
329 manually rotated to search for energetically stable orientation. The candidate structures were

330 pre-optimized using the molecular mechanics method with the MMFF94s force field as  
331 implemented in Avogadro<sup>49)</sup> (version 1.1.1) and then optimized using the DFT method at the  
332 level of  $\omega$ B97X-D/6-31G\*<sup>39)</sup> employing Gaussian09.<sup>50)</sup> The obtained geometries were  
333 characterized as minimum structures on the basis of their harmonic vibrational frequencies and  
334 number of imaginary frequencies.

335

336

### 337 **Acknowledgments**

338 We thank the Screening Committee for Anticancer Drugs supported by a Grant-in-Aid for  
339 Scientific Research on Innovative Areas (“Scientific Support Programs for Cancer Research”)  
340 from the Ministry of Education, Culture, Sports, Science and Technology, Japan.

341 Mass measurements were partly carried out with the JEOL JMS-700 MS spectrometer in  
342 the joint Usage/Research Center (JURC) at the Institute for Chemical Research, Kyoto  
343 University, Japan. The DFT calculations were carried out at the Research Center for  
344 Computational Science, Okazaki National Research Institutes. The NOESY spectrum of **3** was  
345 measured by Dr. Ken-ichi Akagi at the National Institute of Biomedical Innovation (Osaka).

346

### 347 **Funding**

348 This work was partly supported by the Ministry of Education, Culture, Sports, Science and  
349 Technology, Japan under a Grant-in-Aid for Scientific Research on Innovative Areas “Chemical  
350 Biology of Natural Products” [number 23102011] (to KI and RCY), [number 26102733] (to  
351 MA).

352

### 353 **References**

354 [1] Kato Y, Scheuer PJ. Aplysiatoxin and debromoaplysiatoxin, constituents of the marine  
355 mollusk *Stylocheilus longicauda* (Quoy and Gaimard, 1824). J. Am. Chem. Soc.  
356 1974;96:2245–2246.

357 [2] Kikkawa U, Takai Y, Tanaka Y, Miyake R, Nishizuka Y. Protein kinase C as a possible  
358 receptor protein of tumor-promoting phorbol esters. J. Biol. Chem. 1983;258:11442–  
359 11445.

360 [3] Fujiki H, Sugimura T. New classes of tumor promoters: teleocidin, aplysiatoxin, and  
361 palytoxin. Adv. Cancer Res. 1987;49:223–264.

362 [4] Nishizuka Y. Studies and perspectives of protein kinase C. Science. 1986;233:305–312.

- 363 [5] Nishizuka Y. The molecular heterogeneity of protein kinase C and its implications for  
364 cellular regulation. *Nature*. 1988;334:661–665.
- 365 [6] Nishizuka Y. Intracellular signaling by hydrolysis of phospholipids and activation of  
366 protein kinase C. *Science*. 1992;258:607–614.
- 367 [7] Schaar D, Goodell L, Aisner J, Cui XX, Han ZT, Chang R, Martin J, Grospe S, Dudek L,  
368 Riley J, Manago J, Lin Y, Rubin EH, Conney A, Strair RK. A phase I clinical trial of 12-  
369 *O*-tetradecanoylphorbol-13-acetate for patients with relapsed/refractory malignancies.  
370 *Cancer Chemother. Pharmacol.* 2006;57:789–795.
- 371 [8] Fidler B, Goldberg T. Ingenol mebutate gel (picato): a novel agent for the treatment of  
372 actinic keratoses. *P. T.* 2014;39:40–46.
- 373 [9] Pettit GR, Herald CL, Doubek DL, Herald DL, Arnold E, Clardy J. Isolation and structure  
374 of bryostatin 1. *J. Am. Chem. Soc.* 1982;104:6846–6848.
- 375 [10] Szállási Z, Smith CB, Pettit GR, Blumberg PM. Differential regulation of protein kinase C  
376 isozymes by bryostatin 1 and phorbol 12-myristate 13-acetate in NIH 3T3 fibroblasts. *J.*  
377 *Biol. Chem.* 1994;269:2118–2124.
- 378 [11] Szállási Z, Denning MF, Smith CB, Dlugosz AA, Yuspa SH, Pettit GR, Blumberg PM.  
379 Bryostatin 1 protects protein kinase C-d from down-regulation in mouse keratinocytes in  
380 parallel with its inhibition of phorbol ester-induced differentiation. *Mol. Pharmacol.*  
381 1994;46:840–850.
- 382 [12] Wang QJ, Bhattacharyya D, Garfield S, Nacro K, Marquez VE, Blumberg PM.  
383 Differential localization of protein kinase C d by phorbol esters and related compounds  
384 using a fusion protein with green fluorescent protein. *J. Biol. Chem.* 1999;274:37233–  
385 37239.
- 386 [13] Lu Z, Hornia A, Jiang YW, Zang Q, Ohno S, Foster DA. Tumor promotion by depleting  
387 cells of protein kinase Cd. *Mol. Cell. Biol.* 1997;17:3418–3428.
- 388 [14] Reddig PJ, Dreckschmidt NE, Ahrens H, Simsiman R, Tseng CP, Zou J, Oberley TD,  
389 Verma AK. Transgenic mice overexpressing protein kinase Cd in the epidermis are  
390 resistant to skin tumor promotion by 12-*O*-tetradecanoylphorbol-13-acetate. *Cancer Res.*  
391 1999;59:5710–5718.
- 392 [15] Jackson D, Zheng Y, Lyo D, Shen Y, Nakayama K, Nakayama KI, Humphries MJ,  
393 Reyland ME, Foster DA. Suppression of cell migration by protein kinase Cd. *Oncogene.*  
394 2005;24:3067–3072.
- 395 [16] Etcheberrigaray R, Tan M, Dewachter I, Kuiperi C, Van der Auwera I, Wera S, Qiao L,

396 Bank B, Nelson TJ, Kozikowski AP, Van Leuven F, Alkon DL. Therapeutic effects of PKC  
397 activators in Alzheimer's disease transgenic mice. Proc. Natl. Acad. Sci. USA.  
398 2004;101:11141–11146.

399 [17] Gustafson KR, Cardellina JH, McMahon JB, Gulakowski RJ, Ishitoya J, Szallasi Z, Lewin  
400 NE, Blumberg PM, Weislow OS. A nonpromoting phorbol from the Samoan medicinal  
401 plant *Homalanthus nutans* inhibits cell killing by HIV-1. J. Med. Chem. 1992;35:1978–  
402 1986.

403 [18] Wender PA, Verma VA, Paxton TJ, Pillow TH. Function-oriented synthesis, step economy,  
404 and drug design. Acc. Chem. Res. 2008;41:40–49.

405 [19] Kraft MB, Poudel YB, Kedei N, Lewin NE, Peach ML, Blumberg PM, Keck GE.  
406 Synthesis of a des-B-ring bryostatin analogue leads to an unexpected ring expansion of the  
407 bryolactone core. J. Am. Chem. Soc. 2014;136:13202–13208

408 [20] Nakagawa Y, Yanagita RC, Hamada N, Murakami A, Takahashi H, Saito N, Nagai H, Irie  
409 K. A simple analogue of tumor-promoting aplysiatoxin is an antineoplastic agent rather  
410 than a tumor promoter: development of a synthetically accessible protein kinase C  
411 activator with bryostatin-like activity. J. Am. Chem. Soc. 2009;131:7573–7579.

412 [21] Hanaki Y, Kikumori K, Ueno S, Tokuda H, Suzuki N, Irie K. Structure–activity studies at  
413 position 27 of aplog-1, a simplified analog of debromoaplysiatoxin with anti-proliferative  
414 activity. Tetrahedron. 2013;69:7636–7645.

415 [22] Höfle G, Bedorf N, Gerth K, Reichenbach H, inventor; Biotechnolog Forschung Gmbh,  
416 assignee. Epothilone, deren Herstellungsverfahren sowie diese Verbindungen enthaltende  
417 Mittel. German Patent DE 4,138,042, 1993 Oct 14.

418 [23] Bollag DM, McQueney PA, Zhu J, Hensens O, Koupal L, Liesch J, Goetz M, Lazarides E,  
419 Woods CM. Epothilones, a new class of microtubule-stabilizing agents with a taxol-like  
420 mechanism of action. Cancer Res. 1995;55:2325–2333.

421 [24] Borzilleri RM, Zheng X, Schmidt RJ, Johnson JA, Kim SH, DiMarco JD, Fairchild CR,  
422 Gougoutas JZ, Lee FYF, Long BH, Vite GD. A novel application of a Pd(0)-catalyzed  
423 nucleophilic substitution reaction to the regio- and stereoselective synthesis of lactam  
424 analogues of the epothilone natural products. J. Am. Chem. Soc. 2000;122:8890–8897.

425 [25] Hunt JT. Discovery of ixabepilone. Mol. Cancer Ther. 2009;8:275–281.

426 [26] Nakagawa Y, Irie K, Nakamura Y, Ohigashi H. The amide hydrogen of (–)-indolactam-V  
427 and benzolactam-V8's plays a critical role in protein kinase C binding and  
428 tumor-promoting activities. Bioorg. Med. Chem. Lett. 2001;11:723–728.

- 429 [27] Nakagawa Y, Irie K, Masuda A, Ohigashi H. Synthesis, conformation and PKC isozyme  
430 surrogate binding of new lactone analogues of benzolactam-V8s. *Tetrahedron*.  
431 2002;58:2101–2115.
- 432 [28] Song L, Servajean V, Thierry J. Aziridines derived from amino acids as synthons in  
433 pseudopeptide synthesis. *Tetrahedron*. 2006;62:3509–3516.
- 434 [29] Inanaga J, Hirata K, Saeki H, Katsuki T, Yamaguchi M. A rapid esterification by means of  
435 mixed anhydride and its application to large-ring lactonization. *Bull. Chem. Soc. Jpn.*  
436 1979;52:1989–1993.
- 437 [30] Irie K, Oie K, Nakahara A, Yanai Y, Ohigashi H, Wender PA, Fukuda H, Konishi H,  
438 Kikkawa U. Molecular basis for protein kinase C isozyme-selective binding: the synthesis,  
439 folding, and phorbol ester binding of the cysteine-rich domains of all protein kinase C  
440 isozymes. *J. Am. Chem. Soc.* 1998;120:9159–9167.
- 441 [31] Sharkey NA, Blumberg PM. Highly lipophilic phorbol esters as inhibitors of specific  
442 [<sup>3</sup>H]phorbol 12,13-dibutyrate binding. *Cancer Res.* 1985;45:19–24.
- 443 [32] Shindo M, Irie K, Nakahara A, Ohigashi H, Konishi H, Kikkawa U, Fukuda H, Wender  
444 PA. Toward the identification of selective modulators of protein kinase C (PKC)  
445 isozymes: establishment of a binding assay for PKC isozymes using synthetic C1 peptide  
446 receptors and identification of the critical residues involved in the phorbol ester binding.  
447 *Bioorg. Med. Chem.* 2001;9:2073–2081.
- 448 [33] Kishi Y, Rando RR. Structural basis of PKC activation by tumor promoters. *Acc. Chem.*  
449 *Res.* 1998;31:163–172.
- 450 [34] Ganong BR, Loomis CR, Hannun YA, Bell RM. Specificity and mechanism of protein  
451 kinase C activation by *sn*-1,2-diacylglycerols. *Proc. Natl. Acad. Sci. USA.* 1986;83:1184–  
452 1188.
- 453 [35] Kang JH, Chung HE, Kim SY, Kim Y, Lee J, Lewin NE, Pearce LV, Blumberg PM,  
454 Marquez VE. Conformationally constrained analogues of diacylglycerol (DAG). Effect on  
455 protein kinase C (PK-C) binding by the isosteric replacement of *sn*-1 and *sn*-2 esters in  
456 DAG-lactones. *Bioorg. Med. Chem.* 2003;11:2529–2539.
- 457 [36] Nakagawa Y, Irie K, Nakamura Y, Ohigashi H, Hayashi H. Synthesis and biological  
458 activities of indolactone-V, the lactone analogue of the tumor promoter (–)-indolactam-V.  
459 *Biosci. Biotechnol. Biochem.* 1997;61:1415–1417.
- 460 [37] Endo Y, Ohno M, Hirano M, Itai A, Shudo K. Synthesis, conformation, and biological  
461 activity of teleocidin mimics, benzolactams. A clarification of the conformational

462 flexibility problem in structure—activity studies of teleocidins. *J. Am. Chem. Soc.*  
463 1996;118:1841–1855.

464 [38] Irie K, Isaka T, Iwata Y, Yanai Y, Nakamura Y, Koizumi F, Ohigashi H, Wender PA,  
465 Satomi Y, Nishino H. Synthesis and biological activities of new conformationally restricted  
466 analogues of (–)-indolactam-V: elucidation of the biologically active conformation of the  
467 tumor-promoting teleocidins. *J. Am. Chem. Soc.* 1996;118:10733–10743.

468 [39] Chai JD, Head-Gordon M. Long-range corrected hybrid density functionals with damped  
469 atom-atom dispersion corrections. *Phys. Chem. Chem. Phys.* 2008;10:6615–6620.

470 [40] zur Hausen H, Bornkamm GW, Schmidt R, Hecker E. Tumor initiators and promoters in  
471 the induction of Epstein—Barr virus. *Proc. Natl. Acad. Sci. USA.* 1979;76:782–785.

472 [41] Ito Y, Yanase S, Fujita J, Harayama T, Takashima M, Imanaka H. A short-term in vitro  
473 assay for promoter substances using human lymphoblastoid cells latently infected with  
474 Epstein-Barr virus. *Cancer Lett.* 1981;13:29–37.

475 [42] Davies AH, Grand RJ, Evans FJ, Rickinson AB. Induction of Epstein-Barr virus lytic  
476 cycle by tumor-promoting and non-tumor-promoting phorbol esters requires active protein  
477 kinase C. *J. Virol.* 1991;65:6838–6844.

478 [43] Kikumori M, Yanagita RC, Tokuda H, Suzuki N, Nagai H, Suenaga K, Irie K.  
479 Structure-activity studies on the spiroketal moiety of a simplified analogue of  
480 debromoaplysiatoxin with antiproliferative activity. *J. Med. Chem.* 2012;55:5614–5626.

481 [44] Yamori T, Matsunaga A, Sato S, Yamazaki K, Komi A, Ishizu K, Mita I, Edatsugi H,  
482 Matsuba Y, Takezawa K, Nakanishi O, Kohno H, Nakajima Y, Komatsu H, Andoh T,  
483 Tsuruo T. Potent antitumor activity of MS-247, a novel DNA minor groove binder,  
484 evaluated by an in vitro and in vivo human cancer cell line panel. *Cancer Res.*  
485 1999;59:4042–4049.

486 [45] Monks A, Scudiero D, Skehan P, Shoemaker R, Paull K, Vistica D, Hose C, Langley J,  
487 Cronise P, Vaigro-Wolff A, Gray-Goodrich M, Campbell H, Mayo J, Boyd M. Feasibility  
488 of a high-flux anticancer drug screen using a diverse panel of cultured human tumor cell  
489 lines. *J. Nat. Cancer Inst.* 1991;83:757–766.

490 [46] Sakuma M. Probit Analysis of Preference Data. *Appl. Entomol. Zool.* 1998;33:339–347.

491 [47] van der Spoel D, Lindahl E, Hess B, Groenhof G, Mark AE, Berendsen HJC. GROMACS:  
492 fast, flexible, and free. *J. Comput. Chem.* 2005;26:1701–1718.

493 [48] Wang J, Wang W, Kollman PA, Case DA. Automatic atom type and bond type perception  
494 in molecular mechanical calculations. *J. Mol. Graph. Model.* 2006;25:247–260.

495 [49] Hanwell MD, Curtis DE, Lonie DC, Vandermeersch T, Zurek E, Hutchison GR.  
496 Avogadro: an advanced semantic chemical editor, visualization, and analysis platform. *J.*  
497 *Cheminform.* 2012;4:17.

498 [50] Frisch MJ, Trucks GW, Schlegel HB, Scuseria GE, Robb MA, Cheeseman JR, Scalmani G,  
499 Barone V, Mennucci B, Petersson GA, Nakatsuji H, Caricato M, Li X, Hratchian HP,  
500 Izmaylov AF, Bloino J, Zheng G, Sonnenberg JL, Hada M, Ehara M, Toyota K, Fukuda R,  
501 Hasegawa J, Ishida M, Nakajima T, Honda Y, Kitao O, Nakai H, Vreven T, Montgomery  
502 JA, Jr., Peralta JE, Ogliaro F, Bearpark M, Heyd JJ, Brothers E, Kudin KN, Staroverov  
503 VN, Kobayashi R, Normand J, Raghavachari K, Rendell A, Burant JC, Iyengar SS,  
504 Tomasi J, Cossi M, Rega N, Millam JM, Klene M, Knox JE, Cross JB, Bakken V, Adamo  
505 C, Jaramillo J, Gomperts R, Stratmann RE, Yazyev O, Austin AJ, Cammi R, Pomelli C,  
506 Ochterski JW, Martin RL, Morokuma K, Zakrzewski VG, Voth GA, Salvador P,  
507 Dannenberg JJ, Dapprich S, Daniels AD, Farkas Ö, Foresman JB, Ortiz JV, Cioslowski J,  
508 Fox DJ. *Gaussian 09. Revision D.01.* Wallingford CT: Gaussian, Inc.; 2009.



509 **Table 1.**  $K_i$  values for the inhibition of [ $^3\text{H}$ ]PDBu-binding by aplog-1, **1**, **2**, and **3**.

	$K_i$ (nM)			
	Aplog-1 <sup>a</sup>	<b>1</b> <sup>b</sup>	<b>2</b> <sup>b</sup>	<b>3</b>
$\delta$ -C1B peptide	7.4	> 2,500	> 2,500	520 (19) <sup>c</sup>

510 <sup>a</sup>Cited from ref. 20. <sup>b</sup>Cited from ref. 21.

511 <sup>c</sup>Values in parentheses represent the standard deviation from triplicate experiments.

512 **Figure captions**

513

514 **Fig. 1.** Structures of bryostatin-1, aplysiatoxin, its simplified analogs (**1-3**), teleocidin-B4,  
515 indolactam-V, and its 8-membered analogs.

516

517 **Fig. 2.** Cross-eyed stereo views of possible conformations of **3** (**A-C**) and their relative  
518 energies at the  $\omega$ B97X-D/6-31G\* level. Dashed lines represent hydrogen bonding.

519

520 **Fig. 3.** EBV-EA production induced by TPA, aplog-1, **1**, **2**, and **3**.

521 The percentages of EA-positive cells are shown. Sodium *n*-butyrate (4 mM) was added to all  
522 samples to enhance the sensitivity of Raji cells. Only 0.1% of cells were positive for EA at 4  
523 mM sodium *n*-butyrate. The final concentration of DMSO was 0.4%. Cell viability  
524 exceeded 60%. Error bars show the standard error of the mean ( $n = 3$ ). <sup>a</sup>Cited from ref. 43.  
525 <sup>b</sup>Cited from ref. 21.

526

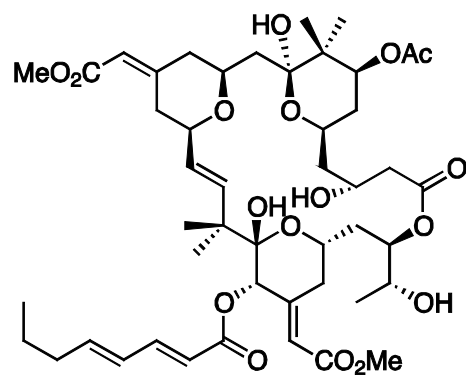
527 **Fig. 4.** Effects of aplog-1, **1**, **2**, and **3** on the growth of human cancer cell lines: HBC-4  
528 (breast) and NCI-H460 (non-small cell lung).

529 Cell growth was expressed as a percentage of the control (media only). The results were  
530 presented as the average of duplicate points.

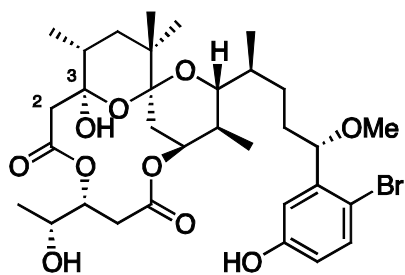
531

532 **Scheme 1.** (a) TFA, dichloromethane (95%); (b) **5**, 2,4,6-trichlorobenzoyl chloride, Et<sub>3</sub>N,  
533 DMAP, toluene (80%); (c) KMnO<sub>4</sub>, NaIO<sub>4</sub>, *t*-BuOH, pH 7 buffer (74%); (d)  
534 *N*-Hydroxysuccinimide, DCC, MeCN; (e) 20% Pd(OH)<sub>2</sub>-C, MeOH (23% in two steps).

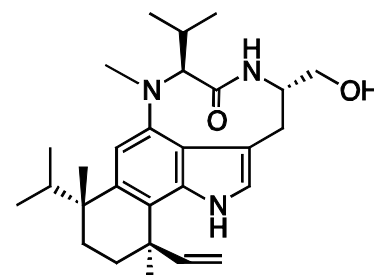
Fig. 1



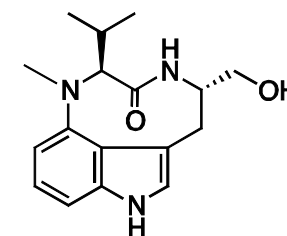
Bryostatin 1



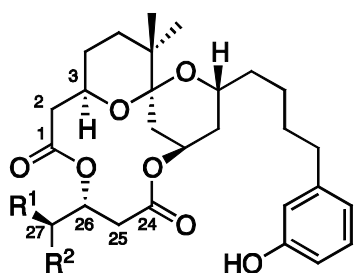
Aplysiatoxin (ATX)



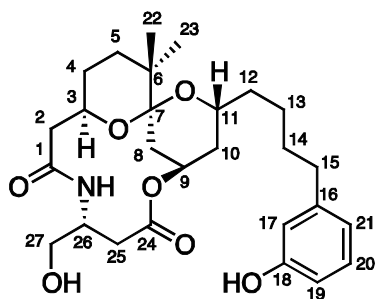
Teleocidin B-4



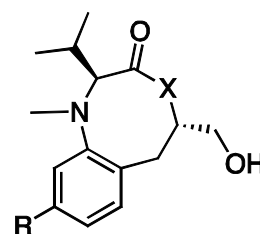
Indolactam-V



- Aplog-1 :  $R^1 = H$ ,  $R^2 = OH$   
1 :  $R^1 = Me$ ,  $R^2 = OH$   
2 :  $R^1 = H$ ,  $R^2 = OMe$

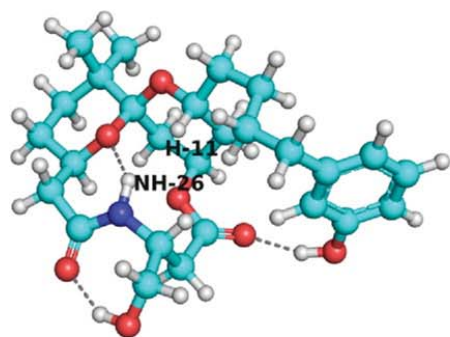


3

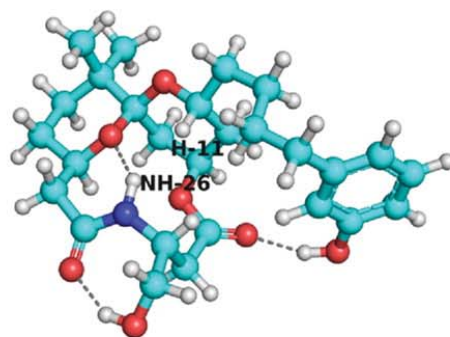


- Benzolactam-V8s :  $X = NH$   
Benzolactone-V8s :  $X = O$

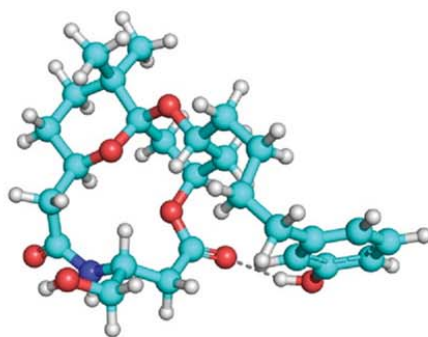
Fig. 2



*trans*-amide form **A**  
0.000 kcal mol<sup>-1</sup>



*trans*-amide form **B** (ATX-like)  
1.365 kcal mol<sup>-1</sup>



*cis*-amide form **C**  
13.259 kcal mol<sup>-1</sup>

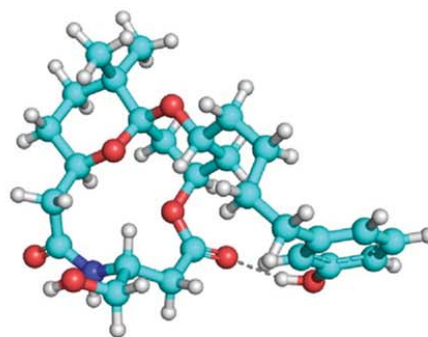


Fig. 3

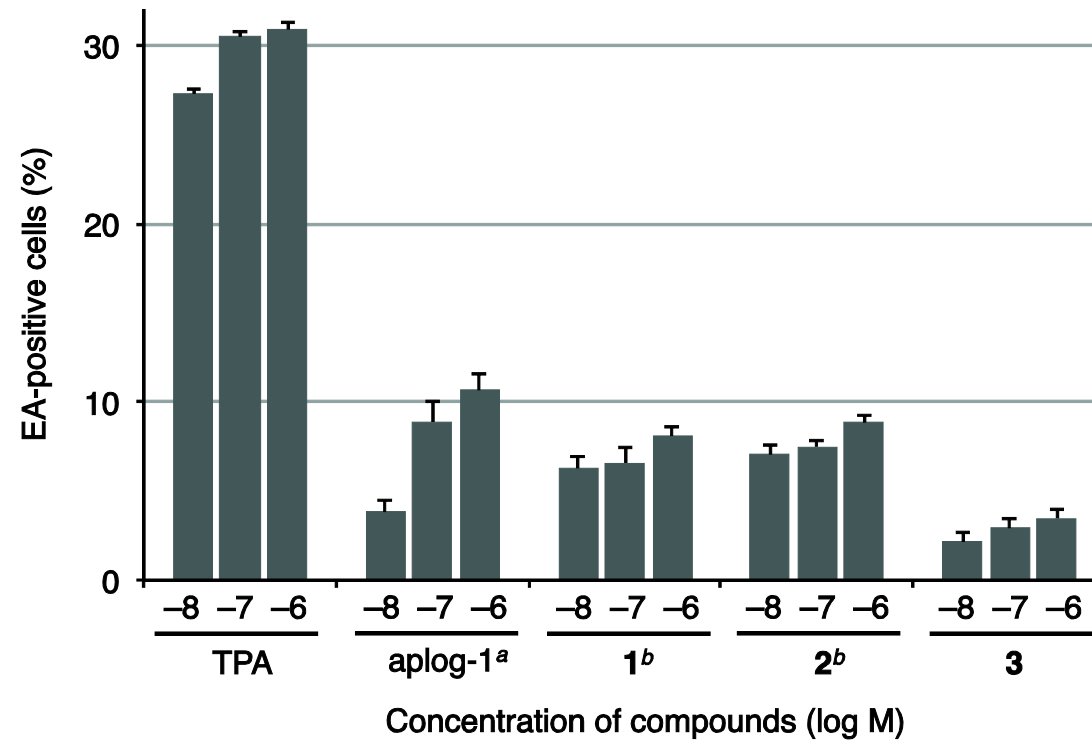
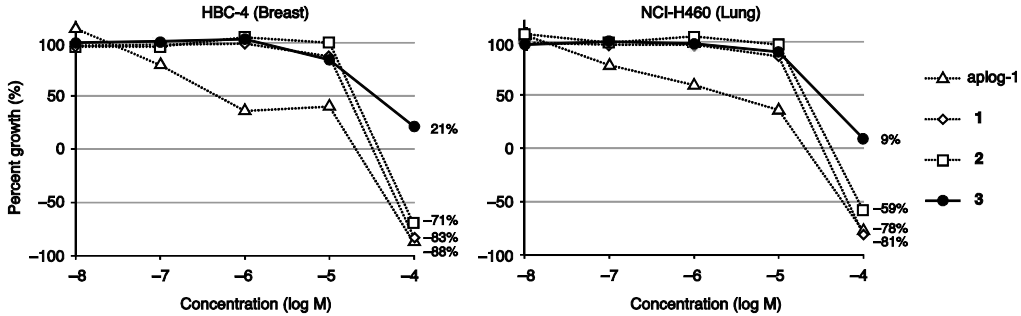
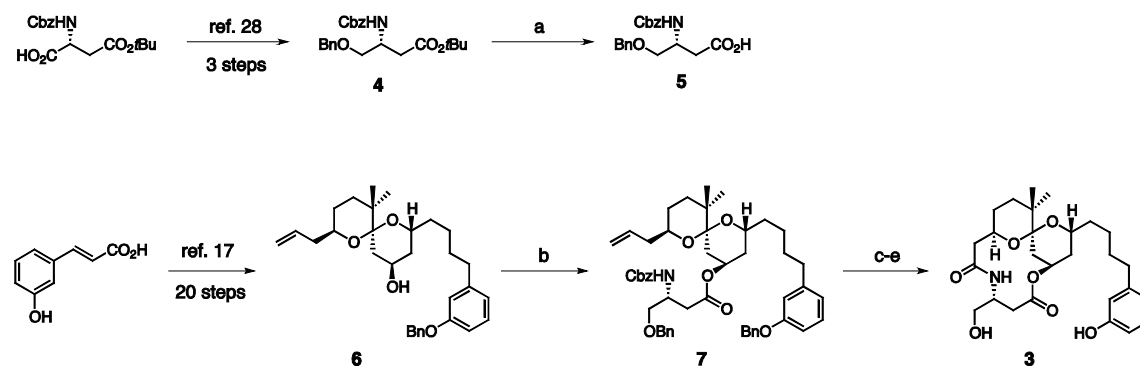


Fig. 4



# Scheme 1



## Supplemental Figures and Table

### Synthesis and biological activities of the amide derivative of aplog-1, a simplified analog of aplysiatoxin with anti-proliferative and cytotoxic activities

Yusuke Hanaki,<sup>1</sup> Ryo C. Yanagita,<sup>1,2</sup> Takahiro Sugahara,<sup>3</sup> Misako Aida,<sup>3</sup> Harukuni Tokuda,<sup>4</sup> Nobutaka Suzuki,<sup>4</sup> and Kazuhiro Irie<sup>\*,1</sup>

<sup>1</sup>*Division of Food Science and Biotechnology, Graduate School of Agriculture, Kyoto University, Kyoto 606-8502, Japan*

<sup>2</sup>*Department of Applied Biological Science, Faculty of Agriculture, Kagawa University, Kagawa 761-0795, Japan*

<sup>3</sup>*Center for Quantum Life Sciences, and Department of Chemistry, Graduate School of Science, Hiroshima University, Higashi-Hiroshima 739-8526, Japan*

<sup>4</sup>*Department of Complementary and Alternative Medicine, Clinical R & D, Graduate School of Medical Science, Kanazawa University, Kanazawa 920-8640, Japan*

#### Contents

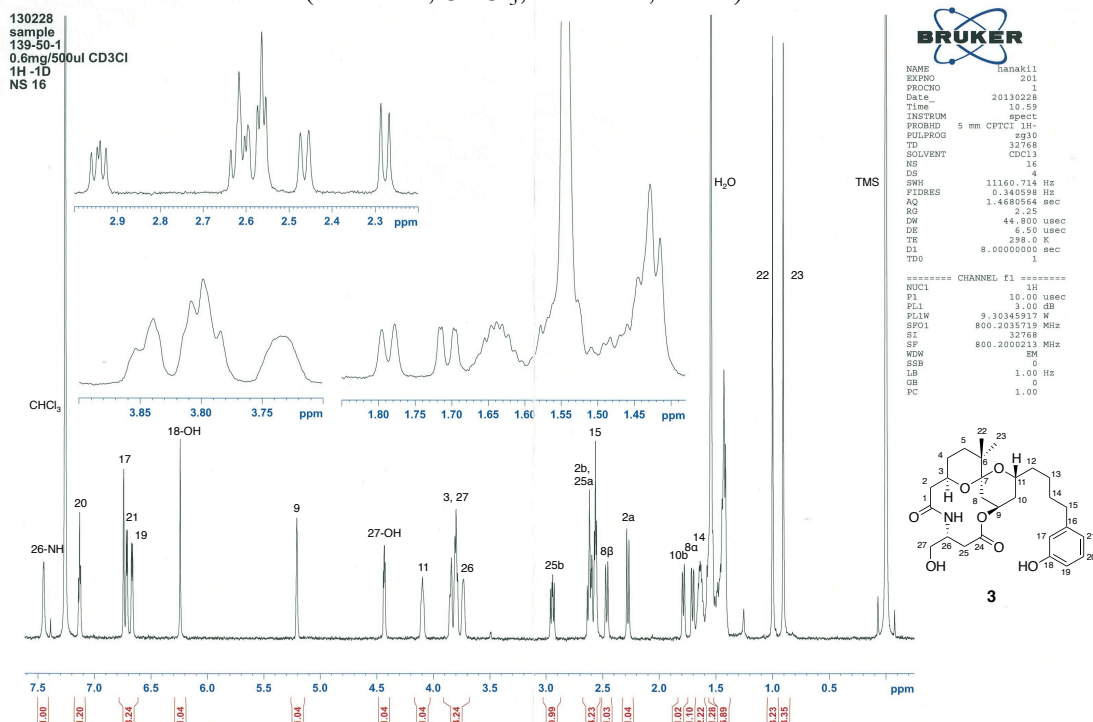
**Supplemental Fig. 1.** <sup>1</sup>H-1D NMR spectrum of amide-aplog-1 (3)

**Supplemental Fig. 2.** 2D <sup>1</sup>H-<sup>1</sup>H NOESY spectrum of amide-aplog-1 (3)

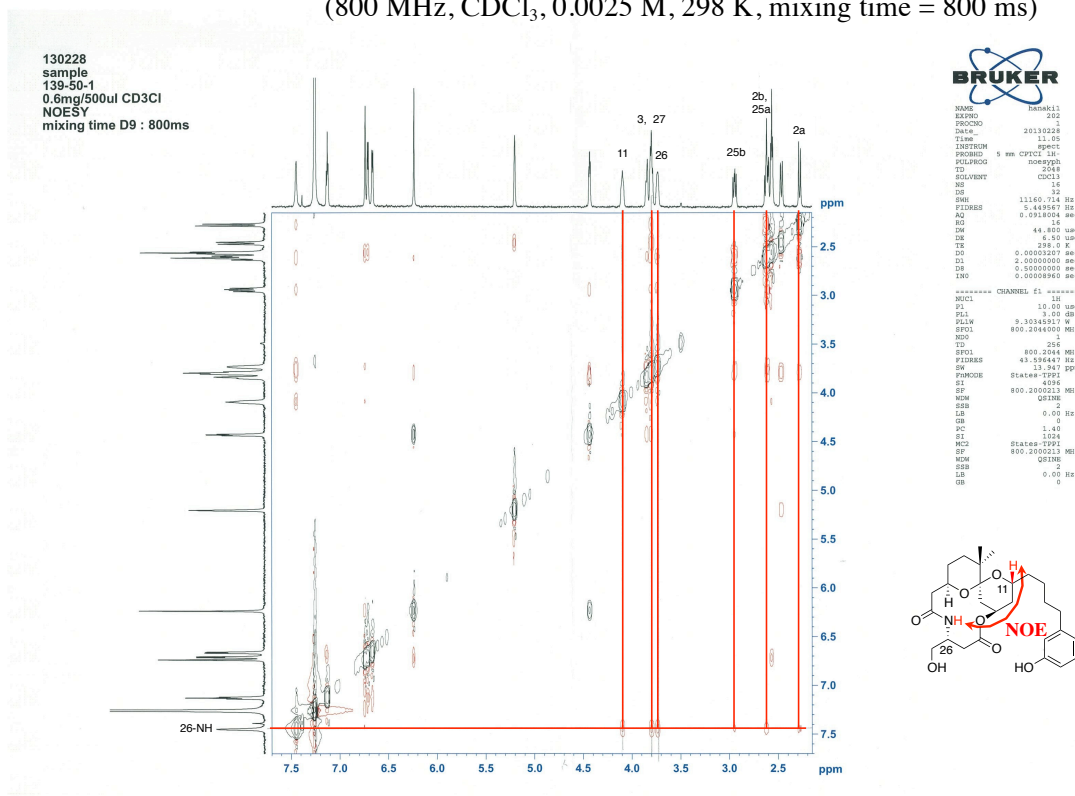
**Supplemental Table 1.** Growth inhibition assay against human cancer cell lines.



**Supplemental Fig. 1.**  $^1\text{H}$ -1D NMR spectrum of amide-aplog-1 (**3**)  
(800 MHz,  $\text{CDCl}_3$ , 0.0025 M, 298 K)



**Supplemental Fig. 2.** 2D  $^1\text{H}$ - $^1\text{H}$  NOESY spectrum of amide-aplog-1 (**3**)  
(800 MHz,  $\text{CDCl}_3$ , 0.0025 M, 298 K, mixing time = 800 ms)



**Supplemental Table 1.** Growth inhibition assay against human cancer cell lines.

cancer cell line		log GI <sub>50</sub> (M)		Cell growth at 10 <sup>-4</sup> M (% of control)			
		Aplog-1 <sup>a</sup>	<b>3</b>	Aplog-1	<b>1</b>	<b>2</b>	<b>3</b>
<b>breast</b>	<b>HBC-4</b>	-6.33	-4.46	-88	-83	-71	21
	BSY-1	-4.87	-4.37	-94	-93	-88	27
	HBC-5	-4.76	-4.20	-85	-84	-92	40
	MCF-7	-4.72	-4.50	-82	-72	-80	8
	<b>MDA-MB-231</b>	-5.61	-4.64	-92	-87	-95	9
<b>CNS</b>	U251	-4.83	-4.47	-89	-93	-81	8
	SF-268	-4.83	-4.31	-83	-87	-72	31
	<b>SF-295</b>	-5.06	-4.54	-80	-61	-67	4
	SF-539	-4.97	-4.37	-84	-75	-81	16
	SNB-75	-4.80	-4.39	-84	-81	-70	17
	SNB-78	-4.72	-4.23	-88	-91	-55	38
<b>colon</b>	<b>HCC2998</b>	-5.43	-4.32	-86	-84	-78	22
	KM-12	-4.86	-4.35	-87	-67	-71	24
	HT-29	-4.77	-4.53	-86	-80	-79	-8
	HCT-15	-4.76	-4.31	-75	-67	-46	28
	HCT-116	-4.79	-4.40	-87	-81	-98	16
<b>lung</b>	NCI-H23	-4.88	-4.26	-75	-68	-71	25
	NCI-H226	-4.81	-4.49	-79	-78	-89	9
	NCI-H522	-4.87	-4.65	-88	-87	-89	-25
	<b>NCI-H460</b>	-5.60	-4.50	-78	-81	-59	9
	<b>A549</b>	-5.32	-4.49	-79	-76	-75	9
	DMS273	-4.90	-4.38	-80	-74	-84	16
	DMS114	-4.79	-4.53	-84	-83	-85	3
<b>melanoma</b>	<b>LOX-IMVI</b>	-5.74	-4.73	-83	-70	-91	-62
<b>ovarian</b>	OVCAR-3	-4.78	-4.48	-84	-85	-78	10
	OVCAR-4	-4.75	-4.35	-85	-87	-94	32
	OVCAR-5	-4.95	-4.00	-93	-87	-96	64
	OVCAR-8	-4.71	-4.35	-73	-62	-80	23
	SK-OV-3	-4.69	-4.22	-96	-67	-40	35
<b>renal</b>	RXF-631L	-4.79	-4.29	-91	-88	-77	29
	ACHN	-4.92	-4.46	-92	-97	-28	8
<b>stomach</b>	<b>St-4</b>	-5.55	-4.39	-84	-72	-72	21
	MKN1	-4.86	-4.26	-81	-76	-90	31
	MKN7	-4.78	-4.44	-87	-59	-60	13
	MKN28	-4.74	-4.43	-63	-62	-71	19
	<b>MKN45</b>	-5.33	-4.31	-89	-61	-43	31
	MKN74	-4.76	-4.43	-79	-69	-78	16
<b>prostate</b>	DU-145	-4.85	-4.29	-86	-68	-62	31
	PC-3	-4.96	-4.41	-65	-69	-56	21
MG-MID <sup>b</sup>		-4.98	-4.40				

<sup>a</sup> Nakagawa, Y.; Yanagita, R. C.; Hamada, N.; Murakami, A.; Takahashi, H.; Saito, N.; Nagai, H.; Irie, K. *J. Am. Chem. Soc.* **2009**, *131*, 7573-7579.

<sup>b</sup> Full panel mean-graph midpoint.